

APPLICATION OF QUASI-STEADY-STATE THERMODYNAMIC MODEL OF CONVENTIONAL HEATING SYSTEM WITH TAKAHASHI CONTROL METHOD

L.Hach and Y. Katoh

Mechanical Engineering, Yamaguchi University, Tokiwadai 2-16-1, Ube, Yamaguchi, 755-8611, Japan

ABSTRACT

An indirect control technique using a single-zone space model is presented. The practice of adjusting temperature of heat supply medium inversely to outdoor air temperature (basic open-loop approach) was replaced with a flux control mechanism and facilitated with Takahashi algorithm¹. In this model a coupling Laplace equation was applied with a non-capacitive nodal net of conductance and the hemisphere surface envelope concept in long-wave radiation calculations. In order to reduce the system's order and make it ready for direct use with DDC techniques used nowadays without requiring an additional math apparatus, the transient responses of the output vector were subjected to approximation instead. The ability of working in a closed control loop was demonstrated using data obtained from middle-long-term temperature measurement at ordinary single-zone spaces during the heating season.

1. INTRODUCTION

Energy for heating in dwellings and administrative buildings requires a significant part of the total energy used yearly during the winter heating season. Beside measures (passive and active) used in building construction, DDC technique is one of the most powerful tools for managing thermal control. In addition, it is gradually becoming a medium or even a short- to long-term investment compared with the development of energy prices³.

There are many conventional heating system installations in buildings without enhanced control devices or with insufficient control devices (such as a steam supply system) or those that are simply not working properly. To correct this, often means carrying out an energy audit to the extent financial resources allow. One such investigation was conducted at an administration building equipped with traditional heaters supplied by steam at temperatures up to 135°C, Fig.1. Rooms are not air-conditioned during the winter heating season, i.e. solely thermal performance of heater units maintains the desired indoor temperature. A chosen (reference) space was investigated for the thermal behavior of an occupied room exposed to winter conditions by

means of a quasi-steady-state model of the room. Overall thermal responses of the space as fundamental scalar functions relate internal and external heat loads to heat fluxes on surrounding walls and sensed heat, removed (or added) through the exchange of ambient air. To obtain pure thermodynamic characteristics of the examined space, unmarked by actual weather conditions and/or internal heat sources (sinks), a model was set up and a series of tests were carried out in order to ensure its structural reliability and validate its parameters. Those matching criteria of Takahashi control formula were extracted from model's structure and further treated as input signals to a PS (proportional-sum) controller. Before doing this, however, an approximation process frequently used in traditional control theory was performed.

Finally, the model was used for controlling the heat flux into the reference room in order to manage desired indoor temperature there by means of an autonomously operating PS controller. The widely used practice of an adjusting (heating medium) input temperature inverse to outdoor air temperature (basic open-loop approach, Adelman 1988) was replaced by heat flux control. The numerical results of the model's output transient functions from simulation tests are well in accord with those obtained from measurement, and proved the model's capability as an alternative for DDC system, if replacement of old type convectors takes place.



Fig.1 Cabinet convector with three row finned-tube heating elements in reference room (heating performance 790 Wm^{-2} under design conditions: steam temperature 375 K; inlet air temperature 291.5 K).

2. MODEL SET UP. SYSTEM BOUNDARY CONDITIONS

2.1 Governing equation. Boundary conditions

Some thermal-process representation may be useful to draw prior writing equations governing the heat transfer process, to view the heat-flow crossing points and avoid redundancy of qualities. The build-up model method here uses the thermal network analog of equivalent RC-circuit elements, Fig.2:

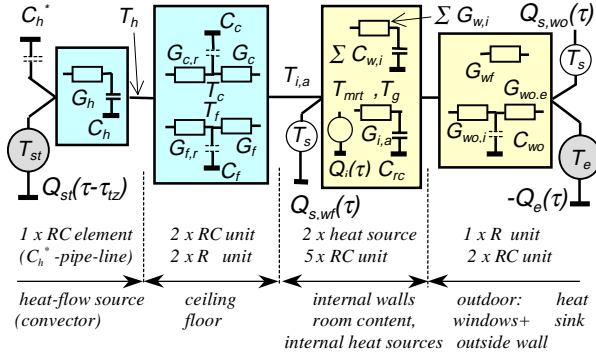


Fig.2 Thermal analog of a single-zone space. Heater (convector) on the left side separated from other internal sources. ($Q_i(\tau)$ -internal heat source, $Q_{s,wf}(\tau)$ -part of solar radiation transmitted through window; $Q_{s,wo}(\tau)$ - part of solar radiation absorbed by outside wall).

Because of very purpose of the structure – to build a ready-for-use model in DDC, selected outputs to sensors and controller have to be determined as well as distinguishing temperature sources (such as any technological devices and, typically, radiation from the sun) from a heat-flow source (convector). In accordance with Fig.2 the heat balance of the enclosed space for accounted heat sources and sinks may be determined as (in specific heat amount per square area unit):

$$dq_h(\tau) = dq_t(\tau) + dq_v(\tau) + dq_{vc}(\tau) - \sum_j dq_{i_j}(\tau) - dq_{s,wo}(\tau) - dq_{s,wf}(\tau) \quad (\text{W.m}^{-2}) \quad (1)$$

j - number of internal heat sources.

The heater has to heat up not only the air volume in the enclosed space, but also the room's contents and the surrounding walls:

$$\sum_{j=1}^6 \left[-m_j c_j \frac{dT_{w,j}(x,\tau)}{d\tau} \right] - m_j c_j \frac{dT_{wo}(x,\tau)}{d\tau} - w \frac{dT_{rc}(y,\tau)}{d\tau} - q_a(\text{W}) \quad (2)$$

Thus, the problem, how a big mass (of walls) acts on an indoor thermal state both by radiation and convection, is apparently shifted to uncertainty over wall thickness (in one-dimensional conduction problem), and for each construction part individually. To get such values with certainty, at least the temperature gradients on both surfaces, best in steady-thermal-state, must be known. These are

specific for each case and must be evaluated through measurement in order to make the calculations reliable. The model features a water equivalent content of the room (w_{rc}), subhourly accounts inputs of heat sources and consequently heat transfer coefficients, and treats both measured temperatures, T_a , T_{mrt} through relations similar to that in [4]. Referring to Fig.2, all heat fluxes involved, except heat exchange by infiltration, could be expressed through boundary conditions on system boundaries. They are set on inner wall surfaces, where the temperatures were also checked. Thus, employing Fourier's law onto isothermal surface parts on:

- outside and internal walls (3a,b),
- windows (3c),
- heater (convector) (3d).

$$-k_{wai} \left[\frac{\partial T_{wo}}{\partial x} \right]_{x=0} = h_{wai}(\tau) [T_{wai}(\tau) - T_a(\tau)] + h_{wai,r}(\tau) \sum_k F_{wak} [T_{wai}(\tau) - T_{wi_k}(\tau)] - \left\{ \frac{1}{A_{tot}} [A_{wo} \alpha_s q_s(\tau) + (1-cv)Q(\tau)] \right\} \quad (3a)$$

$$-k_{wj} \left[\frac{\partial T_{wj}}{\partial x} \right]_{x=0} = h_{wj}(\tau) [T_{wj}(\tau) - T_a(\tau)] + h_{wj,r_j}(\tau) \sum_k F_{wj_k} [T_{wj}(\tau) - T_{wi_k}(\tau)] - \left\{ \frac{1}{A_{tot}} [A_{wj} q_s(\tau) + (1-cv)Q(\tau)] \right\} \quad (3b)$$

$$-k_{wfi} \left[\frac{\partial T_{wfi}}{\partial x} \right]_{x=0} = h_{wfi}(\tau) [T_{wfi}(\tau) - T_a(\tau)] + h_{wfi,r}(\tau) \sum_k F_{wfi_k} [T_{wfi}(\tau) - T_{wi_k}(\tau)] - \left\{ \frac{1}{A_{tot}} [A_{wfi} q_s(\tau) + (1-cv)Q(\tau)] \right\} \quad (3c)$$

$$-k_{hi} \left[\frac{\partial T_{hi}}{\partial x} \right]_{x=0} = h_{hi}(\tau) [T_{hi}(\tau) - T_a(\tau)] + h_{hi,r}(\tau) \sum_k F_{hi_k} [T_{hi}(\tau) - T_{wi_k}(\tau)] - \left\{ \frac{1}{A_{tot}} [A_{hi} Q(\tau) + (1-cv)Q(\tau)] \right\} \quad (3d)$$

The outside wall and window are exposed to the ambient environment's heat fluxes by convection and radiation respectively:

$$-k_{wo,e} \left[\frac{\partial T_{wo}}{\partial x} \right]_{x=s_{wo}} = \alpha q_s(\tau) + h_{wo,e}(\tau) [T_e(\tau) - T_{wo,e}(s_{wo}, \tau)] + h_{wo,e,r}(\tau) \sum_k [T_{e,r}(\tau) - T_{wo,e}(s_{wo}, \tau)] \quad (3e)$$

$$-k_{wf,e} \left[\frac{\partial T_{wf}}{\partial x} \right]_{x=s_{wf}} = \tau w_f q_s(\tau) + h_{wf,e}(\tau) [T_e(\tau) - T_{wf,e}(s_{wf}, \tau)] + h_{wf,e,r}(\tau) \sum_k [T_{e,r}(\tau) - T_{wf,e}(s_{wf}, \tau)] \quad (3f)$$

Similarly, passage space on the opposite side of the outside wall would be considered (heat exchanges with others adjacent rooms were negligible since they are heated on the same temperature regime):

$$-k_{waj} \left[\frac{\partial T_{waj}}{\partial x} \right]_{x=s_{waj}} = h_{waj}(\tau) [T(s_{waj}, \tau) - T_{adj}(\tau)] + h_{waj,r_j}(\tau) \sum_k F_{waj_k} [T_{waj}(\tau) - T_{wi_k}(\tau)] + w_{adj} \frac{\partial T_{adj}}{\partial \tau} - \left\{ \frac{1}{A_{tot}} [A_{waj} \alpha_s q_s(\tau) + (1-cv)Q(\tau)] \right\} \quad (3g)$$

The equation system (3a)-(3g) relates individual heat flows in and from enclosed area and evaluates them for any thermal steady-state or at least quasi-steady state, and provides boundary values for coupling Laplace equations at each part considered isotropic.

2.2 Single-zone space model (SIZO) and Coupling Laplace equations.

Set of dif. equations (3) was put into the state-form of matrices **A** - matrix of dynamics, **B** - matrix of inputs, **C** - state-form matrix, with vectors **u**, **x**, and **y**, respectively (**D** = **0**). At first gradients were separated on the left, multiplied with thermal diffusivity so allowing them to be substituted with (one-dimensional) Laplace equations. As a result, 'unit' Biot numbers are included in matrix of dynamics **A** of dimension 12x12, here displayed are elements $a_{1,1}, a_{1,2}, \dots, a_{1,12}$:

$$\left\{ \begin{array}{l} -a_{wo} \frac{h_{woj}}{k_{woj}} + a_{wo} \frac{h_{woj,r}}{k_{woj}} \left(\sum_{j=1}^5 F_{wo,j} + F_{wo,rc} \right); 0; \left(-a_{wo} \frac{h_{woj,r}}{k_{woj}} F_{wo,1} \right) \\ \left(-a_{wo} \frac{h_{woj,r}}{k_{woj}} F_{wo,2} \right); \left(-a_{wo} \frac{h_{woj,r}}{k_{woj}} F_{wo,3} \right); \left(-a_{wo} \frac{h_{woj,r}}{k_{woj}} F_{wo,4} \right) \\ \left(-a_{wo} \frac{h_{woj,r}}{k_{woj}} F_{wo,5} \right); 0; 0; 0; 0; -a_{wo} \left(\frac{h_{woj,r}}{k_{woj}} + F_{wo,rc} \right) \end{array} \right\} \quad (4)$$

with the vector of state-form variables:

$$\bar{x} = \left[\begin{array}{l} T_{wo,i}; T_{wo,e}; T_{wi_1}; T_{wi_2}; T_{wi_3}; T_{wi_4}; T_{wi_5}; T_{wi_5,e}; \\ T_{wf}; T_{st,o}; T_h; T_a \end{array} \right]^T \quad (5)$$

Disturbances with controlled variable are separated and form the input vector **u** (r=9):

$$\bar{u} = [T_{st,i}; T_{adj,a}; T_{adj,mrt}; T_{a,e}; v T_{a,e}; q_{s,wo}; q_{s,wf}; Q_i; wd]^T \quad (6)$$

with matrix of inputs **B** (9x9):

$$\left\{ \begin{array}{l} 0; 0; 0; 0; 0; \frac{f_{wo} A_{wo}}{k_{woj} A_{tot}}; \frac{f_{wf} A_{wo}}{k_{woj} A_{tot}}; \frac{(1-cv)}{k_{woj} A_{tot}}; 0 \\ 0; 0; 0; 0; 0; \frac{f_{wj} A_{wj}}{k_{wj} A_{tot}}; \frac{f_{wj} A_{wj}}{k_{wj} A_{tot}}; \frac{(1-cv)}{k_{wj} A_{tot}}; 0 \\ 0; 0; 0; 0; 0; \frac{f_{wf} A_{wf}}{k_{wf} A_{tot}}; 1 - \alpha_{wf}; \frac{(1-cv)}{k_{wf} A_{tot}}; 0 \\ 0; 0; 0; 0; 0; \frac{f_h A_h}{k_h A_{tot}}; \frac{f_h A_h}{k_h A_{tot}}; \frac{(1-cv)}{k_w A_{tot}}; 0 \\ 0; 0; 0; 0; -\frac{h_{wo,e}}{k_{wo,e}}; 0; 0; \frac{\alpha_{wo,e}}{k_{wo,e}}; 0; -\frac{f_{wd} h_{wo,e}}{k_{wo,e}} \\ 0; 0; 0; 0; -\frac{h_{wf,e}}{k_{wf,e}}; 0; 0; \frac{\alpha_{wf,e}}{k_{wf,e}}; 0; -\frac{f_{wd} h_{wf,e}}{k_{wf,e}} \\ 0; -\frac{h_{w_3,e}}{k_{w_3,e}}; -\frac{h_{w_3,e,r}}{k_{w_3,e,r}}; 0; 0; 0; 0; 0; 0 \\ 0; 0; 0; 0; 0; \frac{c_a}{3600(w_{rc} + m_a c_a)}; 0; 0; \frac{cv}{w_{rc} + m_a c_a}; \frac{f_{wd} c_a}{3600(w_{rc} + m_a c_a)} \\ \frac{\dot{m}_{st} c_{st}}{m_h c_h}; 0; 0; 0; 0; 0; 0; 0; 0 \end{array} \right\} \quad (7)$$

Column vector of inputs variables consists of $r = 9$ variables, including only controllable variable input steam temperature $T_{st,i}$ related to the steam pressure (operating pressure 0.33 MPa) P_{st} through $T_{st,i} = f(P_{st})$ with the de facto dictated by the longest one distance boiler – emitter. Other disturbances were obtained either from measurement or meteorological data. Difference $(T_h - T_a)$ determinates required convector's heat output completed by radiant part and difference $(T_{st,i} - T_{st,o})$ for known steam flow rate m ($\text{kg}\cdot\text{s}^{-1}$ or m^3h^{-1}) gives a drop in supplied heat rate. Thermal loads from solar radiation u_6 (outside wall), and u_7 (windows) are calculated from the list of variables⁵ given briefly in Fig.3 (some parameters such as sky darkness or pollution coefficients are not included). Internal heat sources u_8 bear the estimation rate (%) of convective (cv) and radiant (1-cv) shares of heat transfer. Natural infiltration rate and ventilation rate coefficients were estimated⁵, as well as wind influence on them (coefficient f_{wd}). State-form variables were all measured except $T_{wo,e}$, and window (a single-glazed) surface temperature had common value for both, inside as well as outside faced surface ($T_{wf,i} = T_{wf,e}$).

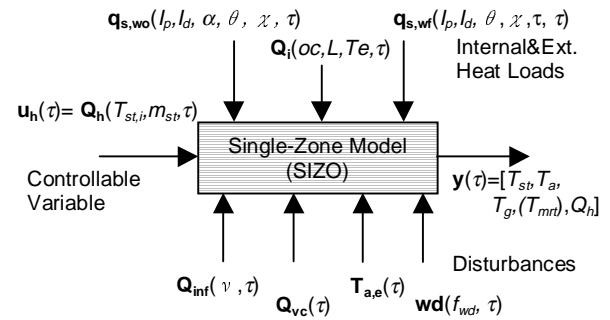


Fig.3 Inputs and outputs of a single-zone model. (oc - number of occupants, L - lights, Te - technological device).

A routine stability check was performed in the process of simulation tests preparations and it was found to be stable for the considered values of matrix **B**(τ). Yet, a value

$$\lim_{t \rightarrow \infty} \int_{t_0}^t \|f^3(t, \tau) B(\tau)\| d\tau \quad (8)$$

$\Phi(t, \tau)$ - transient state-form matrix.

has an upper limit, thus stability of simulation tests depends only on the numerical method itself. While there are non-capacitive terms on the diagonal of matrix **A**, as it will be if the chosen lumpen capacity equations, $\forall a_{ij}, j=1,2,\dots,n$:

$$\{\text{diag} | a_{ij} | < r; r \in \mathbb{R}_x^n; j=1,2,\dots,n\} \quad (9)$$

was satisfied for any r ($r \ll 1$) and is stable within reasonable time step of the numerical method (Runge-Kutta 3.order).

3. THERMAL INERTIA STORAGE AND TIME LAG ESTIMATION

The surroundings walls (with adjacent spaces denoted with subscript ‘adj’ as well as relevant quantities there), are poorly heat-insulated. The outside wall is reinforced concrete with a thin additional plaster (painting cover of thickness 0.3 mm, overall U-value over $3.1 \text{ W.m}^{-2}.\text{K}^{-1}$) – and the single-glazed windows (5 mm, smooth, standard) create unsatisfactory thermal comfort for the occupants. Much of the radiant heat coming in from internal heat sources cannot be re-radiated back into the room and its contents, thus to reach the same level of thermal comfort, the temperature of the indoor air must be increased by convector performance. A ‘two-way’ policy for the SIZO model was adopted to take thermal inertia in:

1. If the outdoor air temperature is low enough, the average heat supply amount depends only on the (steady-state) U-value of outside wall.
2. The room temperature floated above the heating setpoint (22°C) during the measurement period almost always around noon on many days. This excess of energy use above what a steady-state model could predict, resulted in higher thermal losses: each 3 degree excess (with the outside air temperature 0°C) accounts for a 13.6 % increase in heat demand. For such conditions the heat storage ability to absorb a portion of the internal load was estimated.

Elements of matrix **A** (4) were turned into products containing unit Biot numbers’ terms that have to be differentiated along the spatial variable of the Laplace equation. This is executed on non-convective terms set from the Laplace equation’s gradients, all of them in the first 6 rows corresponding to the floor, ceiling and inner walls without windows. With respect to Biot numbers ($\text{Bi} > 0,1$) to estimate the portion of the surrounding walls which ‘take an active part’ in heat capacity, one may consider:

1. method developed for acquiring thermal storage capacity with creation a some new variable

(Arumi-Noe, 1982), or

2. the other way is searching for a *fictive adiabatic plane* within the wall. Such a plane exists in all locations where the temperature gradient appears to have reached zero (there is no internal heat source in the wall). This may occur only if cascade

$$T_{a,e} < T_w < T_a \quad (10)$$

was somewhat extorted.

If equality occurs at the beginning, just on the inner surface, convective heat transfer diminishes. The radiation exchange between such surface and room content may last for state $T_w \neq T_{rc}$. If a similar situation occurs on the opposite surface, the load becomes isolated both from the enclosed area and outdoors - it becomes ‘locked’ within the wall. In a practical sense, the stored heat potential could be accounted for among heat gains within the enclosure only by lowering the setpoint of the heat emitter below $T_{w,i}$, i.e. $T_{w,i} > T_a$, otherwise transmission heat losses are only reduced. Yet, if the first sign in Eq.(10) turns around, the fictive adiabatic plane moves through the wall. This shift has a double effect on the heat flux: it stops it shortly before crossing the plane and contains the heat still flowing from opposite direction, making it available on this side of the enclosure. Thus, in the case where it reaches just half of single-layer wall’s thickness, it resorts to heat storage on behalf of both sides. Such points can be determined on all lines perpendicular to the wall surface. Once these points are indicated, the created plane virtually separates the ‘active’ wall’s portion, i.e. at the time heat is potentially stored, and further defines the other temperature (the first known is on the surface) by which will be finally set the average temperature surface gradient $\left[\frac{\partial T_{wo}}{\partial x} \right]_{x=0}$, resp. $\left[\frac{\partial T_{wi}}{\partial x} \right]_{x=0}$.

Each wall was subjected to the above described procedure and the values of the temperature gradients were determined through a simple computational model, as in Fig.4, used on the outside wall (6 nodes, accuracy $\pm 10\%$):

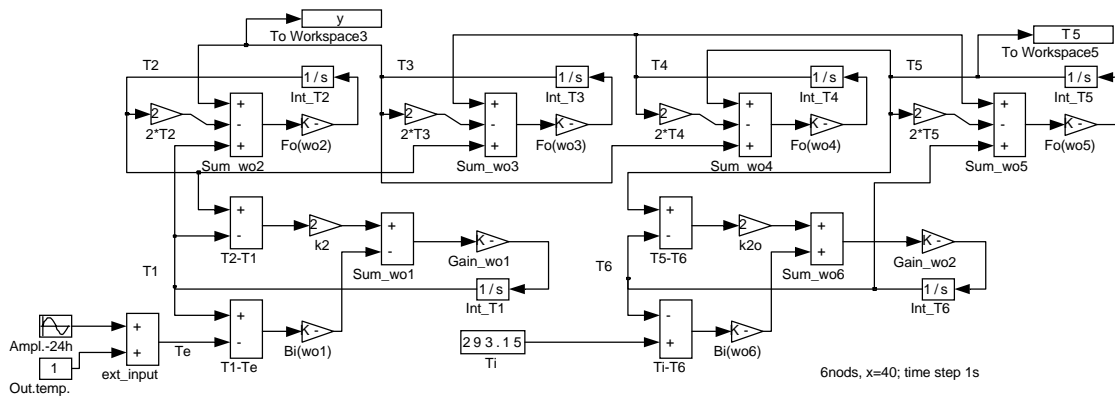


Fig.4. Analog of outside wall temperature distribution with convective boundary conditions.

Surface and nodal temperatures within the k -wall linked through relation

$$T_{w,i}(\tau) = f[T_{w,j}(x, \tau)], \quad j=1,2,\dots,7 \quad (\text{K}) \quad (11)$$

are calculated for material properties (a , k) and boundary values ($h_{w,i}, h_{w,e}$) set at the start of calculation. The transient responses of the temperature distribution within outside wall using a 6-node model is shown in Fig.5. The outside wall was exposed to a distinct 24-hour outdoor temperature swing (curve a , Fig.5). The wave of temperature changes moves from the outside faced surface, creating and pushing the boundary of the no-exchange zone back to the opposite wall surface. At the point P ($\tau = 4,22 \cdot 10^4$ s) the available thermal storage capability is 'cut' 20%. Substituted into Eq. (11) the 'new' wall dimension, resp. thickness x_{adp} could be found. The new value of x_{adp} replaces the previous integration limit value in matrix \mathbf{A} prior to performing new calculations on the SIZO model.

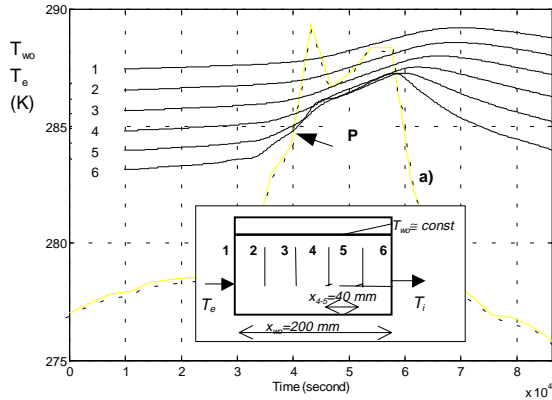


Fig.5 Outside wall temperature distribution (curves 1-6) with combined boundary conditions exposed to outside temperature change (275,9...289,4 K), curve a .

Time lag

A PS controller would require a time parameter, containing information of the system's most difficult to control part, which is obviously any mass associated with heat thermal storage capability and thermal resistance. One may look for reciprocal numbers of eigen values ⁶ in the first 6 equations of matrix \mathbf{A} , or obtain it from simulation tests ⁵. The last option was used, and temperature gradients, heat fluxes, temperature damping, and time lag, respectively, were simultaneously calculated. Instead of an aggregation method ⁶ aimed at reducing system order, method of the gradual integration allowed to check system's constant from two following steady or quasi-steady states. The outside wall alone was subjected to daily outdoor air temperature changes and investigated for any time lag there. The value goes out for any quasi-steady thermal state reached between two corresponding locations on surfaces facing each other on the opposite sides of outside wall:

$$-k_{w,o,e} \left[\frac{\partial T_{wo}}{\partial x} \right]_{x=s_{wo}} = -k_{w,o,i} \left[\frac{\partial T_{wo}}{\partial x} \right]_{x=0} \quad (12)$$

as initial condition. A harmonic signal was used as the input, Fig.6, and time lag was about 2500s.

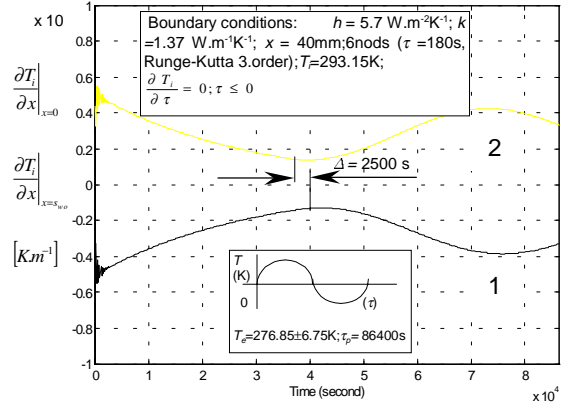


Fig.6 Temperature gradients on out-faced surface (1) and room-faced surface (2) of 200 mm thick outside wall with time lag ($\tau_u \sim 2500$ s) in response to 24-hours-long harmonic input signal (outside air temperature).

Some instability in the beginning of the calculation was deliberately caused by inputting initial values without their derivatives being distant from the immediate vicinity of any steady-state operating points, Fig.6 left. However, this did not affect the accuracy of following numerical calculation in any way (determined only by the method itself, Runge-Kutta 3.order). It demonstrates the range of the dynamic model's stability and reflects positioning its eigen values far from the imaginary axis on a complex plane.

4. PS CONTROLLER IN CLOSED LOOP. CONTROLLER PARAMETERS SETTING

There are no individual control means (dampers or valves) on the side of cabinet convectors, Fig.1, in the whole building. The central steam pressure control takes place only in the heat exchange station's boiler. Steam flow rates into each distribution sub-net were set by throttles at the time of installation and revised during maintenance periods. The efficiency of a secondary control on indoor temperature was demonstrated on the SIZO model connected to the direct, deterministic, parameter control system. For evaluation of the closed loop object-controller was used Laplace transformation in continuous space

$$L(x(\tau)) = x(p) \quad (13)$$

and utilizing generalized notation of the closed-loop feedback control system with an object – the SIZO model (transient function $\mathbf{F}_s(p)$) and PI controller (tr.f. $\mathbf{F}_c(p)$), Fig.7:

$$\frac{L\{y\}}{L\{u\}} = \frac{F_s(p)}{1 + F_s(p) \cdot F_R(p)} \quad (14)$$

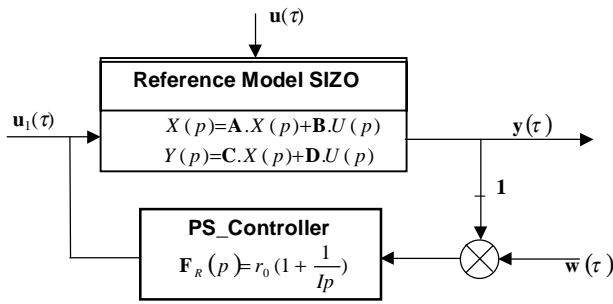


Fig.7 Closed-loop control system with SIZO model.

By means of an unit step input is further obtained transient output, here for unit step disturbance - $u_1(\tau)$:

$$y(p) = \frac{F_s(p)}{1 + F_s(p)r_0(1 + \frac{1}{T_i p})} \cdot \frac{1}{p}$$

$$\therefore y(p) = \frac{K_1}{(p^3 + K_2 p^2 + K_3 p + K_4) + K_1 r_0 (1 + \frac{1}{T_i p})} \cdot \frac{1}{p} \quad (15)$$

$K_j, j=1,2,3,4$ – model coefficients.

In such a form, all necessary tests on the proposed SIZO model were conducted to verify its reliability and accuracy, respectively. In comparing the model's outputs, real data measurement was satisfied on most critical tests, including transient responses on harmonic input signals modeling a 24-hours temperature swing, Fig.6, and allowed us to reduce the model's order. Thus prepared, the reference model was put into the closed control-loop system with a controller in order to generate model error e_m and thus to adjust the actual controller's parameters, i.e. *controller gain* and *integral constant*. As initial values, Eq. (16), (17), served measured data, temperature responses t_{mrt} , t_a with time lag τ_u , transient time τ_n and system gain K .

Controller Parameters Settings

For perpetual tuning of the PS controller *Takahashi algorithm*² was employed. Its requirements are not critical as long as the sampling period is short enough, i.e. much less then SIZO model's time constants themselves. Takahashi method has to be viewed as analogy to the Ziegler-Nichols method for PS controllers. The recommended values for tuning the controller parameters (integral time const. and gain):

$$r_0 K = \frac{0,9 \cdot \tau_n}{\tau_u + \frac{\Delta \tau}{2}} - \frac{0,135 \cdot \tau_n \cdot \Delta \tau}{\left(\tau_u + \frac{\Delta \tau}{2}\right)^2} \quad (16)$$

$$\frac{\Delta \tau}{T_i} = \frac{0,27 \cdot \tau_n \cdot \Delta \tau}{r_0 K \left(\tau_u + \frac{\Delta \tau}{2}\right)^2}$$

where

τ_i – integral time constant (s) $\Delta \tau$ - sampling period (s)
 τ_u - time lag (s) τ_n - transition time (s)
 r_0 – (controller) gain (-) K – (system) gain (-)

substituting $R = K/\tau_n$, $K_p = r_0$, $K_I = r_0 \cdot \Delta \tau / \tau_i$ and $\Delta \tau \ll \tau_s$:

$$K_p = \frac{0,9}{R \left(\tau_u + \frac{\Delta \tau}{2}\right)} - \frac{1}{2} K_I \quad (17)$$

$$K_I = \frac{0,27 \cdot \Delta \tau}{R \left(\tau_u + \frac{\Delta \tau}{2}\right)^2}$$

Controller gain and its integral constant, resp. parameter K_I were tuned into the values in Tab.1, where values recommended by Ziegler-Nichols and the difference in % between both method are shown:

Tab.1 Controller parameters (Takahashi method and method Ziegler-Nichols).

Parameter	Sym-bol	Dimen-sion	TAKA-HASHI	ZIEGLER-NICHOLS	Difference
Proport. constant (gain)	r_0	-	29,0	36,1	19,7
Integral time constant	τ_i	s (h)	9 050 (2,5)	8 400 (2,3)	7,7%
Integral constant	K_I	-	2,88	3,87	25,5
Sampling period	$\Delta \tau$	S	900	900	-

For simulation tests a flexible non-continuous (digital) controller with proportional and sum components, i.e. discrete analogy of normal PI controller (PS type) served:

$$u(k) = r_0 \left[e(k) + \frac{\Delta \tau}{T_i} \sum_{i=0}^k e(k) \right] \quad (18)$$

The controller evaluates the model error, Fig.8, next page, and adds correcting signal Δu_1 (Fig.9) to the SIZO model input u_1 maintaining the temperature difference on convector necessary to keep the prescribed indoor temperature (22°C).

5. SETTING OF NEW WORKING POINT OF CONTROLLER

The controller can be set into a multitask regime. While the SIZO model represents almost all rooms on one half of the building, with exception of some rooms in the 1st floor, obtaining a new transient response, Eq. (15) in each space prior to setting the heater's temperature was necessary. The new calculation of the controller's parameters K_p and K_I precedes the new outcome when the closed-loop is disconnected as in point 1, Fig.7. Thus the new value of output $y(\tau)$ was calculated, and its constants τ_u and

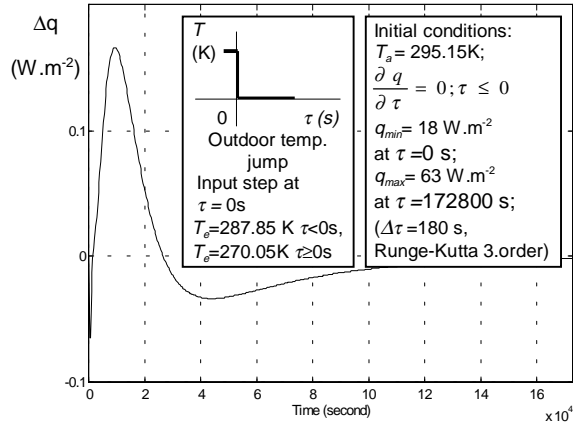


Fig.8 Model error of heat flux. Input variable to PS controller in response to outdoor temperature jump (287,9...270,1 K) at time $\tau = 0$ (s).

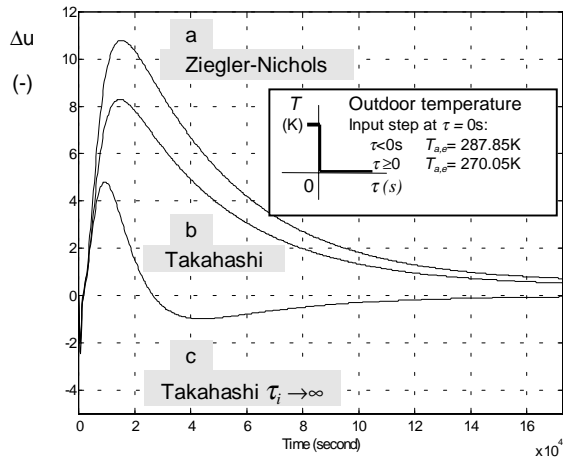


Fig.9 PS-controller output. a – Ziegler-Nichols, b – Takahashi, c – Takahashi with K_i turned off. Controller evaluates new increment $\Delta u_1(\tau) = f(T_h - T_a)$ from the right side of Eq. (1) at the each step of sampling time ($\Delta\tau = 900$ s).

τ_n defined the controller's parameters, Eq. (16), resp. (17). Their calculations were performed after evaluation of the new transient function $y(\tau)$. In order to keep the trajectory of the output vector $\mathbf{y}(\tau)$ near to the desired value $\mathbf{y}_a(\tau)$ it means we must formulate a restrictive condition for its outcome, i.e. move within its vicinity's boundaries. In a state-space platform that intends to seek a minimal value of output vectors track:

$$\min I = \sum_{k=0}^{\infty} e^2(k) \quad (19)$$

$$\text{where } e(k) = w(k) - y(k); \quad k = j \cdot \Delta\tau, \quad j = 0, 1, 2, \dots$$

or including (measured) disturbances ⁷:

$$\min \Phi(y_j, u_j) = \frac{1}{2} \sum_{j=0}^{\infty} (y_j - \bar{y})' Q (y_j - \bar{y}) + (u_j - \bar{u})' R (u_j - \bar{u}) \quad (20)$$

Eq. (19) is the minimizing criteria function (a variation of ordinary time-continuous control

quality square integral form $I_s = \int_0^{\infty} e^2(\tau) d\tau$), that was

found to be satisfied with Takahashi's settings with the integral constant turned out, Fig.9, curve c.

In equation (20) \mathbf{u} is the r -vector of manipulable inputs, $\forall \mathbf{u} \in \mathbf{R}_u^r$, \mathbf{y} is the p -vector of measurable outputs, $\forall \mathbf{y} \in \mathbf{R}_p^p$, and matrices \mathbf{Q} and \mathbf{R} are symmetric positive definite. This procedure involves handling temperature differences $\Delta = T_{st,i} - T_{st,o}$, if flux is being controlled and the output vector must be enlarged for one more variable.

6. CONCLUSIONS

There are a relatively large number of solutions in the field of thermal comfort control approaches for enclosed spaces, partly because of many well designed models themselves⁸, and partly because of the widespread continuing development of new control strategies and control methods⁹. The priorities of this model were focused on a few goals aiming at lowering model's order and being ready-for-use with any PS (PI) controller, without requiring any other tools for closing the control loop. Linear terms in the matrix of dynamics were involved in long-wave radiation calculation, but stopped short of doing so in the expression of convection parameters, issued from studies in natural convection. On the other hand, there was a demand to handle first order differential equations involving coupling Laplace equations, evaluation of the SIZO model time constant simultaneously with the sampling time, and demand on real-time calculation of the output from the controller (term $\mathbf{u}_1(\tau)$).

1. Takahashi algorithm seems to fit to control circuits, where system being controlled may have $\tau_u/\tau_n > 0,2$.
2. The sampling time, shorter than any of the SIZO model's time constants, including transport delay τ_{td} , may be restricted only by Shannon theorem applied on all components of vector $\mathbf{u}(\tau)$. The model would comply well to an ordinary shaped room and use would not be restricted to a single-zone space, in that the surrounding walls could 'see' each other (without convex edges).
3. While controlling heat flux emitted from the convector, the integral function of the PI (PS) controller becomes of less importance and its time constant may be set in a wide range without substantive loss of accuracy. If enlarged enough to be satisfied $\tau_n, \tau_n \ll \tau_i$, the accuracy of the heat flux being controlled drops about 1.8% compared to the full PS settings given in table 1. Takahashi algorithm is suitable for corrections of an inaccurately set heating curve and its immediate correction in case of quick changes of heat fluxes (discontinuing heating regime and direct solar radiation). The adjustments of both the controller's

parameters, integral constant K_i and gain K_r , could be made for each room once, or once in a while simultaneously with the calculation of the model's outputs' $\mathbf{y}(\tau)$ at the sampling time frame $\Delta\tau$, or one can opt for longer intervals.

ACKNOWLEDGEMENTS

Authors would like to thank our colleagues for their assistance during collecting data from measurement, and namely Dr.Y.Isobe for provided experimental devices and Mr.Y.Yamashita for technical help.

REFERENCES

- [1] Takahashi, Y., "The theory of dynamical systems controlled by computers (translation)", The Technical Sciences, Publishing Company, Tokyo, 1974.
- [2] 高橋安人: 「デジタル制御」. 件名 NDLSH: 制御理論, 出版者 東京: 岩波書店, 出版年 1985.3, (in Japanese).
- [3] U.S. Department of Energy, "Review of Microcomputer Residential Energy Analysis Software Applications. DOE/CE/15156-1". Washington, DC., 1984.
- [4] Dear, de R., "Ping-Pong Globe Thermometers for Mean Radiant Temperatures", H&V Engineer, Volume 60, No 681.
- [5] ASHRAE Handbook of Fundamentals, Chapter 23, 25, 28, Atlanta, 1989a.
- [6] Ménézo, Ch.P., Castanet, S.N. and Roux, J.J., "Simulation of Heat Transfer in Buildings Using Reduced Models Coupled With Non Linearities", Heat Transfer 1998, Proceedings of 11th IHTC, Vol.4, pp.343-348, Kyongju, Korea, August 23-28 1998.
- [7] Rawlings, J.B., "Tutorial Overview of Model Predictive Control", Control Systems, Volume 20, No3, pp.39-52, June 2000.
- [8] Fort, K., "Regulace podlahového vytápení", VVI journal, p.19, No1/1995.
- [9] Firm catalogs Honeywell, Co. 1999.

NOMENCLATURE

a thermal diffusivity ($\text{m}^2 \cdot \text{s}^{-1}$)
 A surface area (m^2)
A, B,
C, D state-space model matrixes
 c specific heat ($\text{J} \cdot \text{K}^{-1} \cdot \text{kg}^{-1}$)
 f distribution coefficient (-)
 F radiant comprehend factor (-)
 ($F = \varepsilon \cdot \sigma \cdot F_g \cdot A$)
F transfer function

h heat transfer coefficient ($\text{W} \cdot \text{m}^{-2} \cdot \text{K}^{-1}$)
 k thermal conductivity ($\text{W} \cdot \text{m}^{-1} \cdot \text{K}^{-1}$)
 K controller parameter (-)
 (K_p – proportional, K_i – integral)
 m steam flow rate ($\text{W} \cdot \text{kg}^{-1}$), ($\text{kJ} \cdot \text{m}^{-3} \cdot \text{s}^{-1}$),
 mass (kg)
 p Laplace variable
 q heat flux per unit surface area ($\text{W} \cdot \text{m}^{-2}$)
 Q heat flux (W)
 r_o controller gain
 s (wall) thickness (m)
 T thermodynamic temperature ($^\circ\text{K}$)
 t temperature ($^\circ\text{C}$)
 w water equivalent of (reference room) content
 per unit wall area ($\text{J} \cdot \text{m}^{-2} \cdot \text{K}^{-1}$),
 (spatial) dimension (m)
 $\mathbf{u}, \mathbf{x}, \mathbf{y}$ state-space variable (vector)

Greek alphabet

α absorptivity (-)
 ε emissivity (-)
 θ temperature (non-dimensional),
 solar altitude angle ($^\circ$)
 ν ventilation rate (-)
 ρ density ($\text{kg} \cdot \text{m}^{-3}$)
 σ Stefan-Boltzmann constant
 τ time (s), transmissivity (-)
 τ_i controller's integral time constant (s)
 τ_u/τ_n ratio of time constants (-)
 (τ_u - time lag (s), τ_n - transition time (s))
 $\Delta\tau$ sampling time (s)
 \varkappa azimuth of (vertical) wall ($^\circ$)

Indexes

a air
 adj adjacent (room)
 c ceiling
 cv convective
 cd conductive
 f floor
 g globe, geometrical (factor)
 h heater
 i indoor, internal
 inf infiltration
 hms hemispheric envelope
 max maximal
 min minimal
 mrt mean radiant temperature
 o outdoor
 r radiant
 rc room content
 s solar, system (chapt.4, 5)
 st steam
 td transport time delay (s)
 tot total
 v infiltration
 vc controlled ventilation
 w wall
 wd wind
 wf window